Nanoscale Res Lett (2010) 5:1093–1101
DOI 10.1007/s11671-010-9607-0

NANO EXPRESS

Barium Titanate Nanoparticles: Highly Cytocompatible Dispersions in Glycol-chitosan and Doxorubicin Complexes for Cancer Therapy

Gianni Ciofani · Serena Danti · Delfo D'Alessandro · Stefania Moscato · Mario Petrini · Arianna Menciassi

Received: 28 February 2010 / Accepted: 6 April 2010 / Published online: 9 May 2010

Abstract In the latest years, innovative nanomaterials have attracted a dramatic and exponentially increasing interest, in particular for their potential applications in the biomedical field. In this paper, we reported our findings on the cytocompatibility of barium titanate nanoparticles (BTNPs), an extremely interesting ceramic material. A rational and systematic study of BTNP cytocompatibility was performed, using a dispersion method based on a non-covalent binding to glycol-chitosan, which demonstrated the optimal cytocompatibility of this nanomaterial even at high concentration (100 μg/ml). Moreover, we showed that the efficiency of doxorubicin, a widely used chemotherapy drug, is highly enhanced following the complexation with BTNPs. Our results suggest that innovative ceramic nanomaterials such as BTNPs can be realistically exploited as alternative cellular nanovectors.

G. Ciofani (✉) · A. Menciassi
Center of MicroBioRobotics c/o Scuola Superiore Sant'Anna, Italian Institute of Technology, Viale Rinaldo Piaggio 34, 56025 Pontedera (Pisa), Italy
e-mail: g.ciofani@sssup.it; gianni.ciofani@iit.it

S. Danti · D. D'Alessandro · M. Petrini
CUCCS-RRMR, University of Pisa, via Roma 55, 56126 Pisa, Italy

D. D'Alessandro · S. Moscato
Department of Human Morphology and Applied Biology, University of Pisa, Via Roma 55, 56126 Pisa, Italy

M. Petrini
Department of Oncology and Transplants, University of Pisa, Via Roma 55, 56126 Pisa, Italy

A. Menciassi
Scuola Superiore Sant'Anna, Viale Rinaldo Piaggio 34, 56025 Pontedera (Pisa), Italy

Keywords Barium titanate nanoparticles · Glycol-chitosan · Doxorubicin · Neuroblastoma · Cancer therapy

Introduction

Delivery systems for therapeutics range from liposomal complexes to particles made up of various materials, including ceramics, polymers and metals [1–3]. Among the chemotherapy drugs, there has been an extensive interest for doxorubicin [4], a cytotoxic anthracycline antibiotic that works by intercalating with DNA to interfere with nucleic acid synthesis, producing a marked effect on cells in the *S* phase of cell cycle and affecting DNA transcription [5]. Moreover, doxorubicin is a fluorescent molecule with a chromophore group composed of three planar and aromatic hydroxyanthraquinonic rings, and its intrinsic fluorescence is exploited to monitor its accumulation in living systems [6].

Although used frequently, a major problem associated with doxorubicin administration involves its side effects, in particular concerning cardiac function, myelosuppression, alopecia and hepatic toxicity [7–9]. Interesting advances to reduce side effects involved the development of a targeted approach to chemotherapy through a liposomal system, available as Doxil [10]. However, its safety has constantly been under investigation due to the adverse side effects still experienced by patients [11, 12]. Thus, there is still necessity for the development of improved systems for doxorubicin administration [13–16].

In this paper, we described an alternative and previously unreported supramolecular complexation of doxorubicin with a ceramic nanomaterial, barium titanate nanoparticles (BTNPs), that might be exploited for cancer therapy. Ceramic materials based on perovskite-like oxides are of

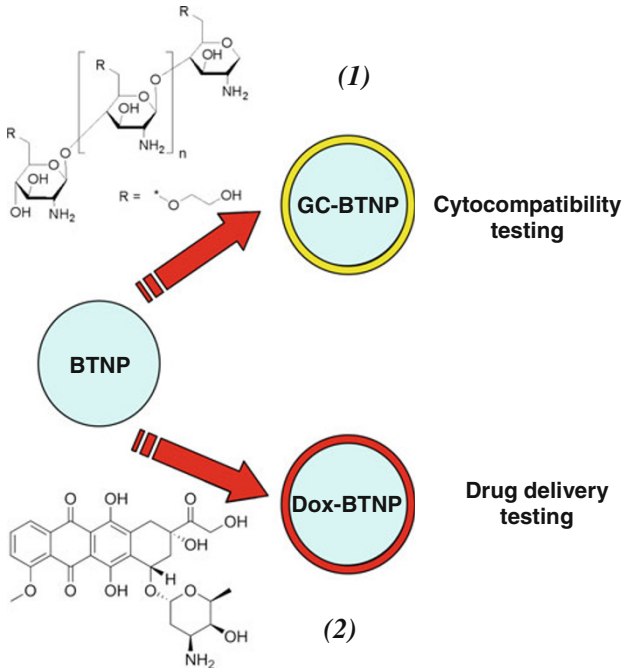

Fig. 1 Schema of the preparation of the BTNPs for biological testing

intense interest because of their applications in electrical and electronic devices [17]. Due to its high dielectric constant, barium titanate ($BaTiO_3$) is probably one of the most studied compounds of this family [18]. No evidence of bio-applications of this nanomaterial has been found in the literature to our knowledge, so we first proposed a preliminary in vitro investigation into cytocompatibility and cell interactions of barium titanate nanoparticles [19]. Here, we introduced two non-covalent functionalizations of the nanoparticles (Fig. 1): with (1) glycol-chitosan and (2) doxorubicin.

Glycol-chitosan dispersion is essential to evaluate the cytocompatibility of the nanoparticles not associated with the drug. A polymer wrapping is a useful and effective method to have samples suitable for biological testing, being barium titanate strongly hydrophobic. To this scope, glycol-chitosan, a biopolymer already widely used in the biomedical field [20–22], resulted an excellent solution. As a dispersing agent of absolute biocompatibility [23], glycol-chitosan allowed us to drastically increment the tested concentration of nanoparticles with respect to our previous study, which was performed using poly-L-lysine [19], thus enabling a systematic and rational investigation into cytotoxicity to be performed in a wide range of concentrations (0–100 μg/ml) and throughout several complimentary assays (MTT, Live/Dead, apoptosis and ROS detection).

As a second step, a complexation of BTNPs with doxorubicin was performed that allowed, after administration to neuroblastoma SH-SY5Y cells, a statistically significant increment of the cellular internalization of this drug to be revealed. An increased drug uptake mediated by BTNP nanovectors indicates, at least theoretically, that a reduced dose can be administered, maintaining unaltered the efficiency of the treatment. These results seem to be strictly correlated with the high propensity of BTNPs to be internalized by the cells, as demonstrated by TEM analysis, and thus to a more efficient uptake of the drug, that is non-covalently complexed to the nanoparticles.

Materials and Methods

Cytocompatibility Testing

Preparation of the Samples

Barium titanate nanoparticles (BTNPs) were purchased from Nanostructured & Amorphous Materials, Inc. (Houston, TX). Details of sample purity and composition, as provided by the supplier, include yield 99%; BaO/TiO_2: 0.999–1.001; purity: 99.9%; APS: 100 nm (from scanning electron microscope); SSA: 10–11 m^2/g; color: white; morphology: spherical and true density: 5.85 g/cm^3. After purchasing, BTNP samples were further analyzed in order to show additional characterization. The energy dispersive X-ray analysis [19] confirmed the data provided by the supplier, and no significant impurities were detected by the micro-analysis, with a relative quantitative composition as following: Ba $\sim$ 60%, Ti $\sim$ 18% and O $\sim$ 22%.

Since pristine dry samples of BTNPs appeared as strongly hydrophobic large aggregates, cytocompatibility evaluation was performed after stabilization in an aqueous environment thanks to a non-covalent wrapping with glycol-chitosan (GC; G7753 from Sigma). Dispersions were prepared with phosphate-buffered saline (PBS) solution. Nanoparticles (10 mg) were mixed with 10 ml of a 1 mg/ml GC solution in a polystyrene tube. The samples were sonicated for 12 h (by a Bransonic sonicator 2510) using an output power of 20 W for all the experiments, resulting in a stable GC–barium titanate nanoparticle (GC–BTNP) dispersion by the non-covalent coating with GC (1 mg/ml GC and 1 mg/ml BTNP, 1:1 w/w). Microphotographs of the final dispersion of GC–BTNPs were obtained *via* both focused ion beam microscopy (FIB, FEI 200) and transmission electron microscopy (TEM, Zeiss 902), pipetting a small quantity of a GC–BTNP aqueous sample on a copper grid and let it dry in a 37°C oven.

Particle size distribution of the dispersions was analyzed with a Nano Z-Sizer 90 (Malvern Instrument); each acquisition was performed three times, on samples appropriately diluted in PBS.

Cytocompatibility assays were performed using a human neuroblastoma SH-SY5Y cell line (CRL-2266

from ATCC). Cells were cultured in Dulbecco's modified Eagle's medium (DMEM) and Ham's F12 (1:1 volume ratio) with 10% fetal bovine serum (from ATCC), 100 IU/ml penicillin, 100 μg/ml streptomycin and 2 mM L-glutamine. Cells were maintained at 37°C in a saturated humidity atmosphere containing 95% air/5% CO_2.

MTT Assay

For viability testing, 3-(4,5-dimethylthiazole-2-yl)-2,5-diphenyl tetrazolium bromide (MTT; M2128 from Sigma) cell proliferation assays were carried out. After trypsinization and counting with a hemocytometer, 5,000 cells were seeded in 96-well plate chambers. Once adhesion was verified (about 12 h after seeding), cells were incubated with 0, 5, 10, 20, 50 and 100 μg/ml of GC–BTNPs for 48 h. At each endpoint, cultures were incubated with MTT at 0.5 mg/ml for further 4 h, followed by addition of dimethyl sulfoxide (DMSO; D8418 from Sigma) at 100 μl/well for cell lysis. Then, absorbance was measured with a microplate reader (Victor3, Perkin Elmer) at 550 nm. Appropriate controls were performed by incubating cells with the corresponding concentrations of glycol-chitosan, but without BTNPs.

Viability/Cytotoxicity Test

Cell viability was further investigated with the LIVE/DEAD® viability/cytotoxicity test (Molecular Probes). The kit contains calcein AM (4 mM in anhydrous DMSO) and ethidium homodimer-1 (EthD-1, 2 mM in DMSO/H_2O 1:4 v/v). After incubation for 48 h at a GC–BTNP concentration ranging in 0–100 μg/ml, cells (30,000 in 24-well plate chambers, $n = 3$) were rinsed with PBS and treated for 10 min at 37°C with 2 μM calcein AM and 4 μM EthD-1 in PBS. Cultures were finally observed with an inverted fluorescence microscope (TE2000U, Nikon) equipped with a cooled CCD camera (DS-5MC USB2, Nikon) and with NIS Elements imaging software, equipped with the appropriate filters.

Live cells can be distinguished from dead ones due to the presence of ubiquitous intracellular esterase activity, determined by the enzymatic conversion of the non-fluorescent cell-permeant agent, calcein AM, to an intensely fluorescent molecule, calcein. Calcein is well retained within live cells, producing an intense uniform green fluorescence. Conversely, EthD-1 enters cells with damaged membranes and undergoes a strong fluorescence enhancement upon binding to nucleic acids, thereby producing a bright red fluorescence in dead cells. EthD-1 is excluded by the intact plasma membrane of live cells.

Early Apoptosis Detection

Apoptosis plays a fundamental role in many normal biological processes as well as in several diseased states of cells and can be induced by various stimuli that will further result in systematic cell death. One of the methods employed to study apoptosis detects changes in the position of phosphatidylserine (PS) in the cell membrane. In non-apoptotic cells, most PS molecules are localized on the inner layer of the plasma membrane, but soon after the initiation of apoptosis, PS is redistributed to the outer layer of the membrane and becomes exposed to the extracellular environment [24]. Exposed PS can be easily detected using annexin *V*, a 35.8-kDa protein with strong affinity for PS.

For early apoptosis detection, 30,000 cells were seeded in 24-well plate chambers ($n = 3$) and treated with 0–100 μg/ml of GC–BTNPs for 48 h. ApoAlert kit (Clonetech Laboratories) was used to evaluate differences between normal and apoptotic cells after treatments. The kit contains annexin V-FITC (20 μg/ml in Tris-NaCl), 1× binding buffer and propidium iodide (PI; 50 μg/ml in 1× binding buffer). Cells were rinsed with 1× binding buffer and then incubated with 200 μl of 1× binding buffer containing 5 μl of the annexin V solution and 10 μl of the PI solution; then, 5 μg/ml of Hoechst 33342 (H1399 from Invitrogen) was used for nucleus staining (blue). After incubation in the dark at room temperature for 20 min, cells were observed *via* fluorescence microscopy with the appropriate filters.

The combination of annexin V-FITC with PI, a red fluorescent DNA-intercalating agent excluded by viable cells, allows necrotic (red stained), early apoptotic (green stained), apoptotic (green and red stained) and normal cells (unstained) to be identified.

Reactive Oxygen Species Detection

Generation of reactive oxygen species (ROS) is a normal event for aerobic organisms, and, in healthy cells, occurring at a controlled rate. Under conditions of oxidative stress, like exposure to nanomaterials [25], ROS production is dramatically increased, resulting in subsequent alteration of membrane lipids, proteins and nucleic acids.

ROS production in SH-SY5Y cells treated with GC–BTNPs was detected using the Image-IT Green Reactive Oxygen Species Detection kit (Invitrogen). The assay is based on 5-(and-6)-carboxy-2′,7′-dichlorodihydrofluorescein diacetate (carboxy-H_2DCFDA), a fluorogenic marker for ROS in viable cells. The non-fluorescent carboxy-H_2DCFDA permeates live cells and is deacetylated by non-specific intracellular esterases. In the presence of non-specific ROS (produced throughout the cell, particularly during oxidative stress), the reduced fluorescein compound is oxidized and

emits bright green fluorescence [26]. Cells (30,000 *per* well) were seeded in 24-well plate chambers ($n = 3$) and treated with 0–100 μg/ml of GC–BTNPs for 48 h. Thereafter, they were incubated for 45 min with a 25 μM carboxy-H_2DCFDA working solution (in DMSO:PBS at 1:400 v/v) and immediately observed *via* fluorescence microscopy with the appropriate filters. During the last 5 min of incubation, cell nuclei were blue stained with 5 μg/ml of Hoechst 33342.

Doxorubicin Complexes Testing

Preparation of the Samples

Complexes between doxorubicin and barium titanate nanoparticles were prepared by mixing 10 mg of nanoparticles with 10 ml of a 100 μg/ml aqueous solution of doxorubicin (D1515 from Sigma) followed by sonication of the resulting dispersion for 6 h, as described for the GC–BTNP preparation. The final product is a stable dispersion of BTNPs in doxorubicin (Dox-BTNPs), having concentrations of 1 mg/ml and 100 μg/ml of BTNPs and Dox, respectively. The obtained dispersion was characterized by spectrophotometric analysis, using a LIBRA S12 Spectrophotometer UV/Vis/NIR (Biochrom). Particle size distribution was analyzed as previously described.

MTT Assay

MTT assays, carried out as previously reported, were performed after incubating cell samples (5,000 in 96-well plate chambers, $n = 6$) for 24 h at different concentrations of either Dox-BTNPs or Dox alone. Table 1 summarizes the performed tests that are identified with *K*, *A*, *B*, *C* and *D*, for increasing concentration of Dox-BTNPs. In each test, the ratio doxorubicin:nanoparticles was maintained constant (1:10 w/w), and a respective control with doxorubicin alone (not complexed with the BTNPs) was performed.

Table 1 Summary of the experiments performed on SH-SY5Y with Dox–BTNP complexes and respective controls

Test		Concentrations (μg/ml)	
		[Dox]	[BTNP]
K	Dox	0	0
	Dox–BTNP	0	0
A	Dox	0.5	0
	Dox–BTNP	0.5	5
B	Dox	1	0
	Dox–BTNP	1	10
C	Dox	1.5	0
	Dox–BTNP	1.5	15
D	Dox	2	0
	Dox–BTNP	2	20

For each experiment, concentration of drug and nanoparticles is provided

Dox-BTNP Uptake: Fluorescence Analyses

Cells were treated as reported in previous section for MTT assay. At the endpoint, cultures ($n = 6$) were rinsed three times in PBS and thereafter treated with 100 μl of a 1% Triton X-100 solution (T9284 from Sigma) for 30 min at 37°C. Once complete cell lysis was verified, the sample was transferred in a black 96-well plate for fluorescence measurement on a Victor3 (Perkin Elmer) microplate reader, equipped with the appropriate filters for doxorubicin detection (Ex 485 nm, Em 572).

Cell cultures incubated for 24 h with different concentrations of Dox-BTNPs (and doxorubicin alone as controls) were also imaged with fluorescence microscope.

Dox-BTNP Uptake: TEM Analysis

Internalization of the Dox-BTNP complexes was assessed by TEM. SH-SY5Y cells were seeded at 2×10^6 cells/T25 flask. After adhesion, cell samples were incubated with a Dox-BTNP-modified culture medium (at final concentrations of Dox 1.5 μg/ml and BTNP 15 μg/ml). After a 24-h incubation, samples were washed in PBS 0.1 M, trypsinized and thereafter fixed with 1% w/v glutaraldehyde—4% w/v paraformaldehyde in PBS 0.1 M pH 7.2 for 2 h at 4°C. After washing, the cells were post-fixed in 1% w/v OsO_4 PBS 0.1 M pH 7.2 for 1 h, washed and dehydrated with acidified aceton-dimethylacetal (Fluka) for 10 min. Thus, the samples were mixed in Epon/Durcupan resin in BEEM capsules (#00 from Structure Probe) overnight at room temperature and finally embedded in resin at 56°C for 48 h. Ultrathin sections (20–30 nm thick) were obtained with an Ultrotome Nova ultramicrotome (LKB, Bromma, Sweden) equipped with a diamond knife (Diatome, Biel/Bienne, Switzerland). The sections were placed on 200-square mesh nickel grids, counterstained with saturated aqueous uranyl acetate and lead citrate solutions and observed in a Zeiss 902 transmission electron microscope.

Statistical Analysis

Analysis of data was performed by analysis of variance (ANOVA) followed by Student's *t*-test to test for significance which was set at 5%. MTT and fluorescence tests were performed in esaplicate; all other assays in triplicate. In all cases, three independent experiments were carried out. Results are presented as mean value ± standard error of the mean.

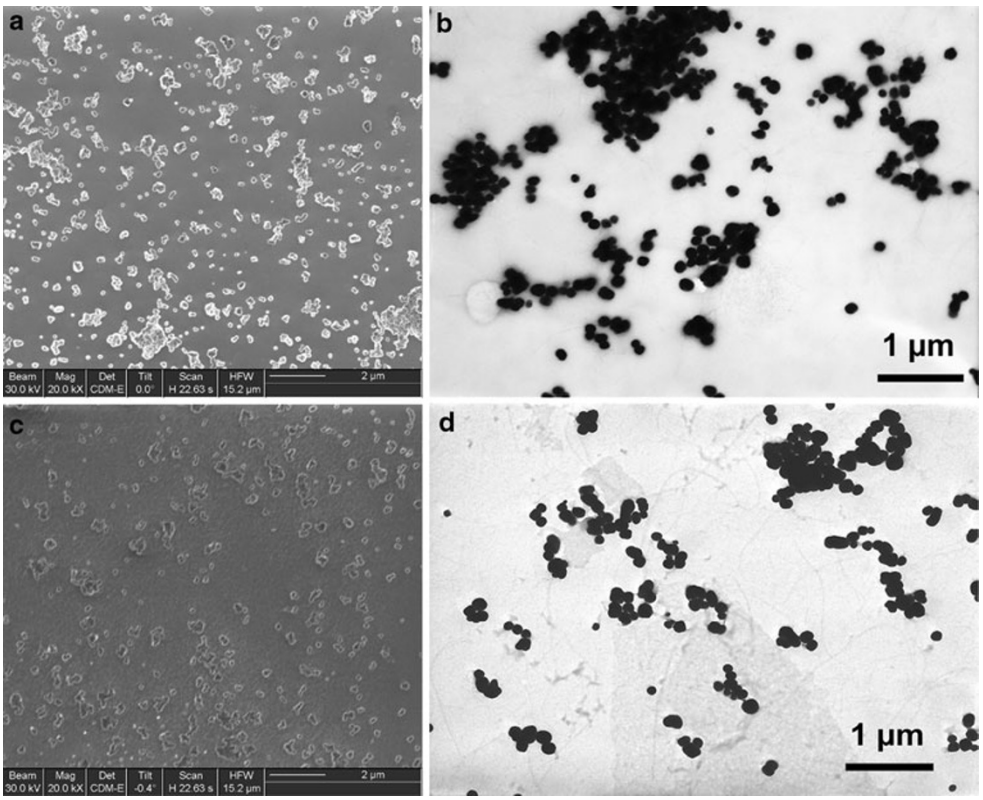

Fig. 2 FIB (**a**, **c**) and TEM (**b**, **d**) imaging of GC–BTNPs (**a**, **b**) and of Dox–BTNPs (**c**, **d**)

Results and Discussion

Evaluation of Cytocompatibility of Glycol-chitosan-Coated Barium Titanate Nanoparticles (GC–BTNPs)

Imaging of the GC–BTNPs by FIB microscopy and TEM revealed well-dispersed structures (Fig. 2a, b), whose sizes were in fully agreement with those obtained by dynamic light scattering analysis, the latter providing a size value of about 285 nm (poly-dispersity index 0.180). After preparation, GC–BTNP dispersions resulted stable for many days, and even if some visible aggregates appeared after 1–2 weeks, they resulted completely dissolvable after a mild sonication (30 min). The dispersions were thereafter appropriately diluted in culture medium for cytocompatibility assessment.

MTT provided an excellent metabolic activity in cells treated up to 100 μg/ml of GC−BTNPs, with a slight decrement in viability at 50 and 100 μg/ml (about 5 and 10%, respectively), from the control, that was not statistically significant in both cases ($p > 0.05$) (Fig. 3).

Cell viability was further investigated with the LIVE/DEAD® viability/cytotoxicity test. Also in this case, the compatibility of GC–BTNPs resulted excellent at each tested concentration (Fig. 4). Absence of cell membrane damage could be detected following cell treatment up to

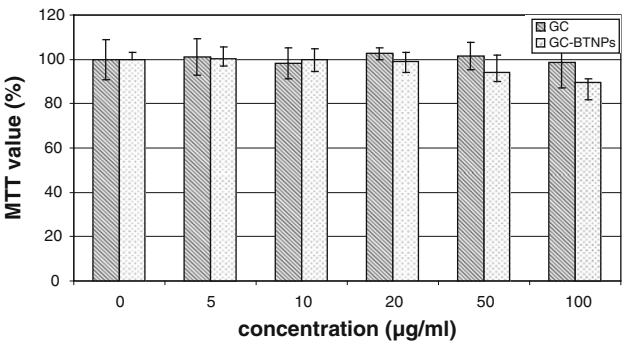

Fig. 3 MTT assay results for increasing GC–BTNPs concentrations and for the respective controls (GC alone)

100 μg/ml of GC–BTNPs, which clearly demonstrates an optimal cell viability, completely comparable to that of the control cultures.

Absence of significant apoptotic phenomena (Fig. 4) was also verified with the annexin V test, and no evidence of apoptosis was observed in all the treated samples. Only a few dead cells could be observed in the sample treated with GC–BTNPs at the highest concentration (100 μg/ml), in agreement with the previous assays.

Finally, ROS production in SH-SY5Y cells treated with GC–BTNPs was analyzed. As shown in Fig. 4, GC–BTNPs do not induce significant oxidative stress after 48-h

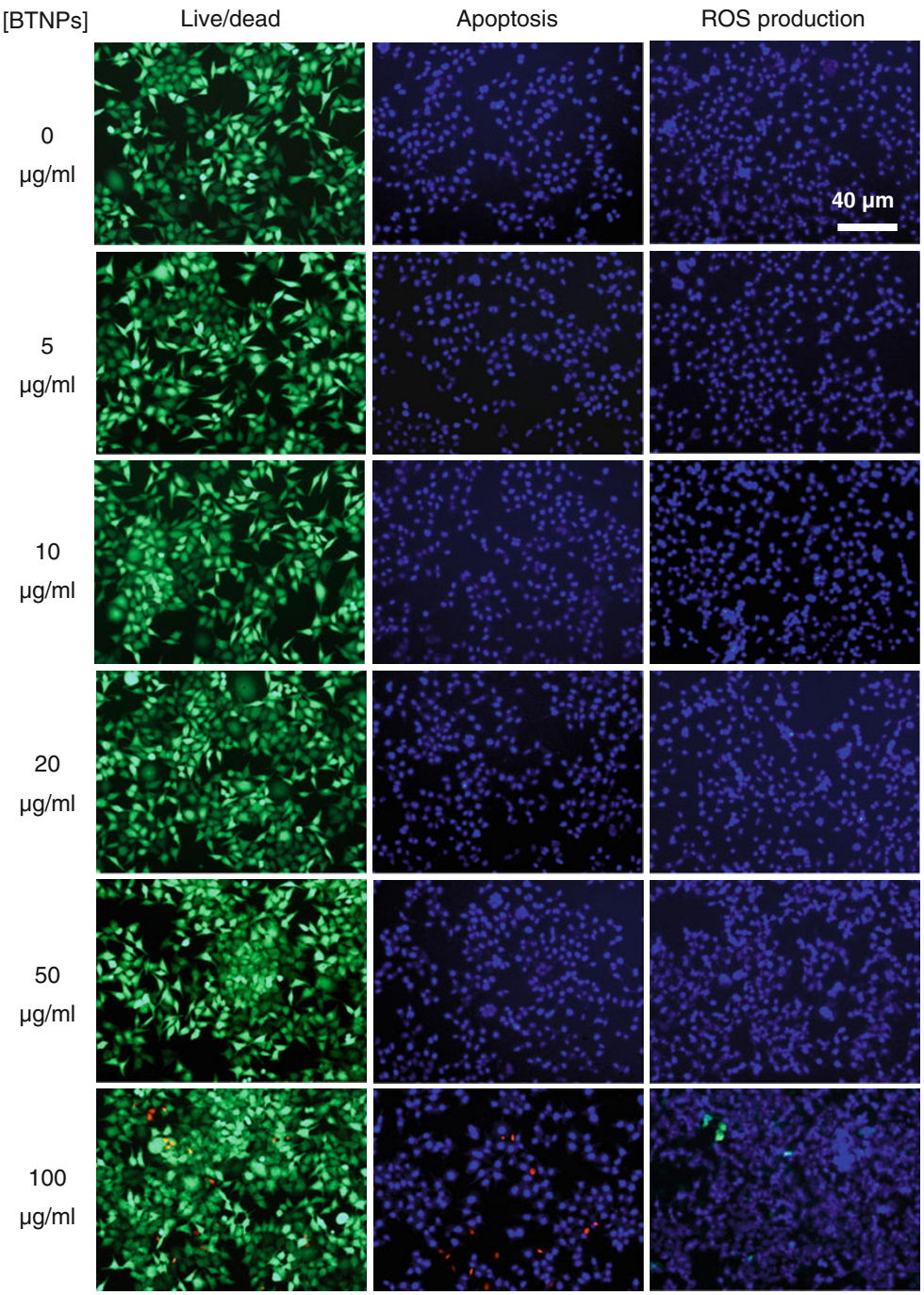

Fig. 4 Summary of the results of the viability/cytotoxicity assay, early apoptosis detection and ROS detection following incubation with increasing GC–BTNPs concentrations

incubation, even at high concentrations, and just a few green-fluorescent cells could be detected at 100 µg/ml concentration, consistent with all the previous cytocompatibility data.

Evaluation of the Efficiency of Dox–BTNP Complexes

Dispersions of BTNPs inside doxorubicin aqueous solutions obviously resulted less stable than those in glycol-chitosan, in particular because of the difference in molecular weight between the polymer and the drug, and therefore of the hydrophobic interactions that stabilize the nanoparticles. Dynamic light scattering analysis showed a bimodal distribution of the sizes, with a first peak around 300 nm (about 20% of the intensity) and a second peak around 2 µm (about 80% of the intensity), denoting the formation of relatively larger aggregates in solution, not directly observable with the FIB (Fig. 2c) and TEM (Fig. 2d) imaging.

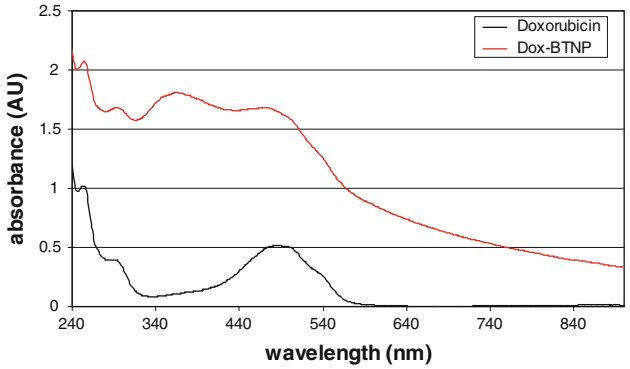

Fig. 5 UV/Vis/NIR absorbance analysis of doxorubicin alone and complexed with the nanoparticles (Dox–BTNP)

Spectrophotometric analysis of the Dox–BTNPs, reported in Fig. 5, confirmed a non-covalent complexation between the doxorubicin and the drug, and spectrum features of doxorubicin are maintained and superposed to the BTNP absorbance, keeping the characteristic peak at 490 nm.

The presence of microaggregates did not prevent the in vitro evaluation of the Dox–BTNP complexes from occurring. Analysis was performed on SH-SY5Y cells at four concentrations, as outlined in Table 1.

Results of Test *A* in treated samples did not differ from those in the control cultures. Cells treated with either doxorubicin alone (500 ng/ml) or doxorubicin complexed with BTNPs (Dox–BTNPs) at a concentration of 5 μg/ml did not reveal any appreciable decrement in viability ($p > 0.1$) with respect to the controls (test *K*). Tests *B* and *C* provided more interesting results. While doxorubicin alone at the tested concentrations (1 and 1.5 μg/ml, in Tests *B* and *C*, respectively) did not show any effects on the neuroblastoma cell proliferation with respect to the controls ($p > 0.1$), when it was combined with BTNPs, the drug efficiency resulted significantly enhanced. Cell viability measured with MTT test achieved a inhibition of about 15% and 20% for concentrations of 10 and 15 μg/ml of Dox-BTNP complexes, respectively (in both cases $p < 0.05$). Also in Test *D*, we noticed a strong increment ($p < 0.005$) in the toxic effects of doxorubicin when combined with the BTNPs (20 μg/ml), although, in this case, also doxorubicin alone (2 μg/ml) was able to considerably inhibit the cell proliferation ($p < 0.05$).

This inhibition increment in cell proliferation in the case of doxorubicin associated with the BTNPs (Fig. 6a) cannot be attributed to a combined toxic effect of nanoparticles and drugs, since in this report we demonstrated the absolute cytocompatibility of the nanoparticles up to a concentration of 100 μg/ml. We can thus hypothesize that the non-covalent complexation of doxorubicin with a nanoparticulate system allows an enhancement of the internalized

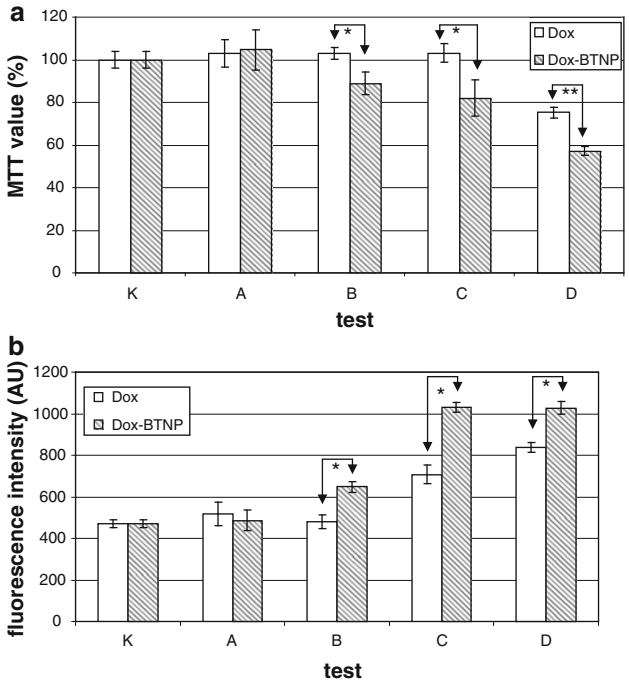

Fig. 6 MTT test (**a**) and fluorescence quantitative uptake investigation (**b**) on the Dox–BTNPs complexes and on respective controls (doxorubicin alone). * $p < 0.05$, ** $p < 0.005$

drug, thanks to a strong uptake of BTNPs by the cells. We therefore investigated the doxorubicin internalized by the cells exploiting the intrinsic fluorescence of this molecule.

Cell lysates of the cultures of Test *K, A, B, C* and *D* were analyzed at appropriate fluorescence wavelengths, and the results are reported in Fig. 6b. The fluorescence values are in agreement with the MTT assay: in Test *A*, we did not observe an appreciable presence of drug internalized by the cells, while Test *B* revealed a statistically significant internalization of doxorubicin (about 40% increment in fluorescence, $p < 0.05$) when doxorubicin (1 μg/ml) is combined with the nanoparticles (10 μg/ml). Internalization of doxorubicin alone, at this concentration, is negligible ($p > 0.05$). Tests *C* and *D* confirmed a strong internalization of the drug, at both concentrations (1.5 and 2 μg/ml, respectively, $p < 0.05$ calculate with respect to the control), that is much more enhanced by the complexation with the nanoparticles: in Test *C* the uptake increment of drug following incubation with Dox–BTNPs was about 80% ($p < 0.05$), while in Test *D* it was about 40% ($p < 0.05$).

These quantitative results were confirmed by fluorescent microscopy. Figure 7 shows cell culture images of Test *C*: Fig. 7a depicts a culture incubated with 1.5 μg/ml of doxorubicin for 24 h, while Fig. 7b depicts the culture treated for the same period with the same concentration of doxorubicin but complexed with the BTNPs (Dox–BTNPs at 15 μg/ml): the increment in red fluorescence in the cells

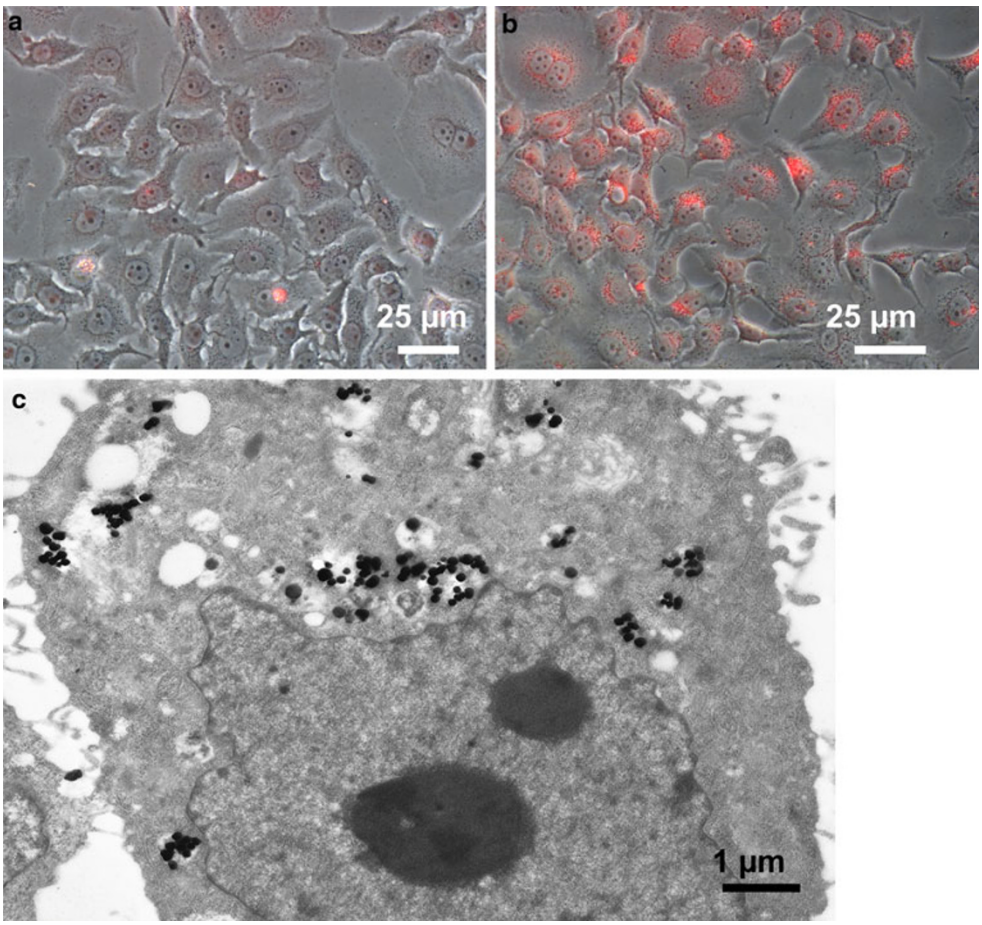

Fig. 7 SH-SY5Y culture incubated for 24 h with 1.5 μg/ml of doxorubicin (**a**) and culture treated for the same period with the same concentration of doxorubicin but complexed with the BTNPs (Dox–BTNPs 15 μg/ml (**b**); TEM imaging on Dox–BTNPs-treated cells (**c**)

is dramatic when the drug is combined with the nanoparticles. These results corroborate the fluorescence quantification previously presented.

All these data confirm an enhancement of the drug uptake by the cells and therefore of the efficiency of doxorubicin when complexed to the BTNPs, most probably due to an increment in drug internalization favoured by the nanoparticles uptake: TEM imaging, in fact, performed after 24 h of incubation in a 15 μg/ml Dox–BTNP-modified medium, confirmed a strong internalization of Dox–BTNPs in the cytoplasm of the SH-SY5Y cells, as shown in Fig. 7c, where the strong-dark electron-dense BTNPs are easily observable in the cells.

Conclusion

In this paper, we have presented two non-covalent approaches for the stabilization of BTNPs in an aqueous environment. Glycol-chitosan, thanks to its cytocompatibility and biological inertia, allowed highly concentrated BTNP dispersions to be obtained that enabled us to extend our previous investigations into BTNP cytotoxicity and to demonstrate the absence of negative effects on cell cultures following the treatment with high concentrations of BTNPs (100 μg/ml).

Additionally, the functionalization with doxorubicin demonstrated the possibility to obtain non-covalent supramolecular complexes, presumably thanks to hydrophobic interactions between the nanoparticle surface and the aromatic rings of the drug. The internalization by the neuroblastoma cells of the drug by exploiting such complexes resulted significantly higher than that obtained using mere doxorubicin solution. Dox–BTNP complexes exhibited considerably enhanced cytotoxic activity when compared to that of doxorubicin alone.

Similar results were recently achieved by other groups with carbon nanotubes [27, 28]. However, we would like to stress that: (i) in our system, we do not require additional surfactants to stabilize the nanostructures and doxorubicin acts *per se* as a stabilizing agent, thus potential toxicity due to high concentration of surfactant is completely avoided;

(ii) the concerns about cytotoxicity of carbon nanotubes are not yet fully addressed in the literature that often offers contrast conclusions [29, 30], hence the necessity to find alternative suitable nanomaterials. Although several investigations are still due, collectively, our results on BTNPs suggest that they can concur in several biomedical applications, as a valid alternative to the currently investigated nanoplatforms.

Acknowledgments Authors gratefully acknowledge Mr. Carlo Filippeschi (Scuola Superiore Sant'Anna, Pisa, Italy) for his assistance for the FIB imaging, Dr. Matilde Masini (Department of Experimental Pathology BMIE, University of Pisa, Pisa, Italy) for TEM technical support and Mr. Lorenzo Albertazzi (Scuola Normale Superiore, Pisa, Italy) for his kind help during the size distribution analyses.

References

1. O.M. Koo, I. Rubinstein, H. Onyuksel, Nanomedicine: NBM **1**, 193 (2005)
2. M.L. Forrest, G.S. Kwon, Adv. Drug Deliv. Rev. **60**, 861 (2008)
3. M.M. Amiji, Nanomedicine: NBM **2**, 299 (2006)
4. J. Wood, Doxorubicin, in *The cytotoxic Handbook*, 4th edn., ed. by M. Allwood, A. Stanley, P. Wright (Radcliffe Medical Press Ltd, Oxon, UK, 2002), pp. 322–329
5. L.B. Liao, H.Y. Zhou, X.M. Xiao, J. Mol. Struct. **749**, 108 (2005)
6. A.B. Anderson, J. Gergen, E.A. Arriaga, J. Chromatogr B **769**, 97 (2002)
7. L.C. Kremer, E.C. van Dalen, P.A. Voute, P.A. Ann, Oncology **13**, 503 (2002)
8. A. Longhi, S. Ferrari, G. Bacci, S. Specchia, Anticancer Drugs **18**, 737 (2007)
9. P. Elliott, Semin. Oncol. **33**, S2 (2006)
10. Ortho-Biotech. DOXIL®—Doxorubicin HCL liposome injection ortho-biotech, http://www.orthobiotech.com/
11. D. Lorusso, A. Di Stefano, V. Carone, A. Fagotti, S. Pisconti, G. Scambia, G. Ann, Oncology **18**, 1159 (2007)
12. H.D. Dorfman, B. Czerniak, Cancer **75**, 203 (1995)
13. M.L. Tan, A.M. Friedhuber, D.E. Dunstan, P.F.M. Choong, C.R. Dass, Biomaterials **31**, 541 (2010)
14. K.J. Longmuir, S.M. Haynes, J.L. Baratta, N. Kasabwalla, R.T. Robertson, Int. J. Pharm. **382**, 222 (2009)
15. J. Park, P.M. Fong, J. Lu, K.S. Russell, C.J. Booth, W.M. Saltzman, T.M. Fahmy, Nanomedicine: NBM **5**, 400 (2009)
16. J.R. Eisenbrey, O. Mualem Burstein, R. Kambhampati, F. Forsberg, J.B. Liu, M.A. Wheatley, J. Control. Release doi: 10.1016/j.jconrel.2009.12.021
17. D. Hennings, C. Metzmacher, B. Schreinemacher, J. Am. Ceram. Soc. **84**, 179 (2001)
18. M. Buscaglia, V. Buscaglia, M. Viviani, N. Nanni, M. Hanuskova, Eur. Ceram. Soc. **20**, 1997 (2999)
19. G. Ciofani, S. Danti, S. Moscato, L. Albertazzi, D. D'Alessandro, D. Dinucci, F. Chiellini, M. Petrini, A. Menciassi, Colloid. Surface B **76**, 535 (2010)
20. J.M. Yu, Y.J. Li, L.Y. Qiu, Y. Jin, Eur. Polym. J. **44**, 555 (2008)
21. Y.J. Son, J.S. Jang, Y.W. Cho, H. Chung, R.W. Park, I.C. Kwon, I.S. Kim, J.Y. Park, S.B. Seo, C.R. Park, S.Y. Jeong, J. Control. Release **91**, 135 (2003)
22. E.S. Lee, K.H. Park, I.S. Park, K. Na, Int. J. Pharm. **338**, 310 (2007)
23. A. Trapani, J. Sitterberg, U. Bakowsky, T. Kissel, Int. J. Pharm **375**, 97 (2009)
24. S.J. Martin, C.P. Reutelingsperger, A.J. McGahon, J.A. Rader, R.C.A.A. van Schie, D.M. LaFace, D.R. Green, J. Exp. Med. **182**, 1545 (1995)
25. K. Pulskamp, S. Diabatè, H.F. Krug, Toxicol. Lett. **168**, 58 (2007)
26. E.J. Park, J. Choi, Y.K. Park, K. Park, Toxicology **245**, 90 (2008)
27. H. Ali-Boucetta, K.T. Al-Jamal, D. McCarthy, M. Prato, A. Bianco, K. Kostarelos, Chem. Commun. **4**, 459 (2008)
28. Z. Liu, X. Sun, N. Nakayama-Ratchford, H. Dai, ACS Nano **1**, 50 (2007)
29. L. Belyanskaya, S. Weigel, C. Hirsch, U. Tobler, H.F. Krug, P. Wick, Neurotoxicology **30**, 702 (2009)
30. G. Bardi, P. Tognini, G. Ciofani, V. Raffa, M. Costa, T. Pizzorusso, Nanomedicine: NBM **5**, 96 (2009)